

# The supernova remnant G284.3-1.8 and the X-ray binary 1FGL J1018.6-5856

Blagoy Rangelov  
George Washington University

Collaborators:

Brian Williams (NASA GSFC/CRESST/USRA)

Oleg Kargaltsev (George Washington University)

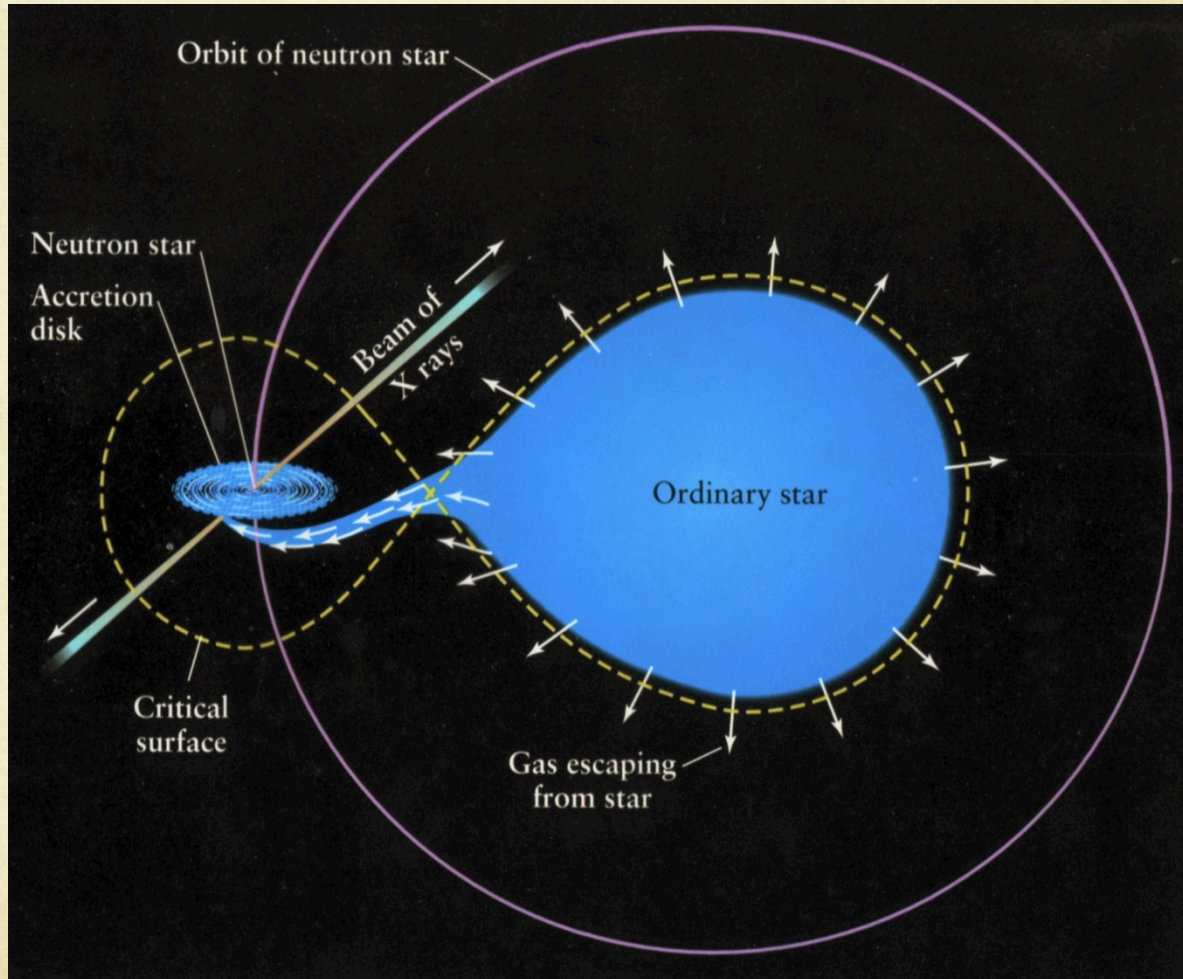
George Pavlov (Pennsylvania State University)

# Outline

- Overview
- Analysis of G284.3-1.8 (G284)
- 1FGL J1018.6-5856 (J1018)
  - Spectral/spatial analysis
  - Binary evolution
- Summary

Based on arXiv:1506.02665 (*in press, ApJL*)

# X-ray Binaries



# Gamma-ray Binaries

Properties of the Known Gamma-Ray Binaries

Source	Detected <sup>a</sup>	$P_{\text{orb}}$ (days)	$e^{\text{b}}$	Compact Source <sup>c</sup>	Companion	$\Gamma_X^{\text{d}}$	Corr. <sup>e</sup>	References
1FGL J1018.6–5856	R, X, G	16.58	...	Pulsar?	O6V((f))	1.44–1.96 <sup>f</sup>	Yes	1, 2, 3
LS 5039	R, X, G, T	3.9	0.35	Pulsar?	O6.5V((f))	1.45–1.61	Yes	4, 5, 6, 7
LS I +61°303	R, X, G, T	26.5	0.55	Pulsar?	Be	1.7–2.0	Yes	8, 9, 10, 11
PSR B1259–63	R, X, G, T	~1240	0.9	Pulsar	Be	1.35–1.83	No	12, 13, 14, 15
Cyg X-3	R, X, G, T	0.2	...	Black hole?	Wolf-Rayet	...	No	16, 17, 18
HESS J0632+057	R, X, T	321	...	Pulsar?	B0pe	1.2–1.6	No	19, 20, 21, 22

## Notes.

<sup>a</sup> Detected energy band. R = Radio, X = X-ray, G = GeV gamma ray, T = TeV gamma ray.

An et al. (2013)

<sup>b</sup> Orbital eccentricity.

<sup>c</sup> Question mark if unconfirmed.

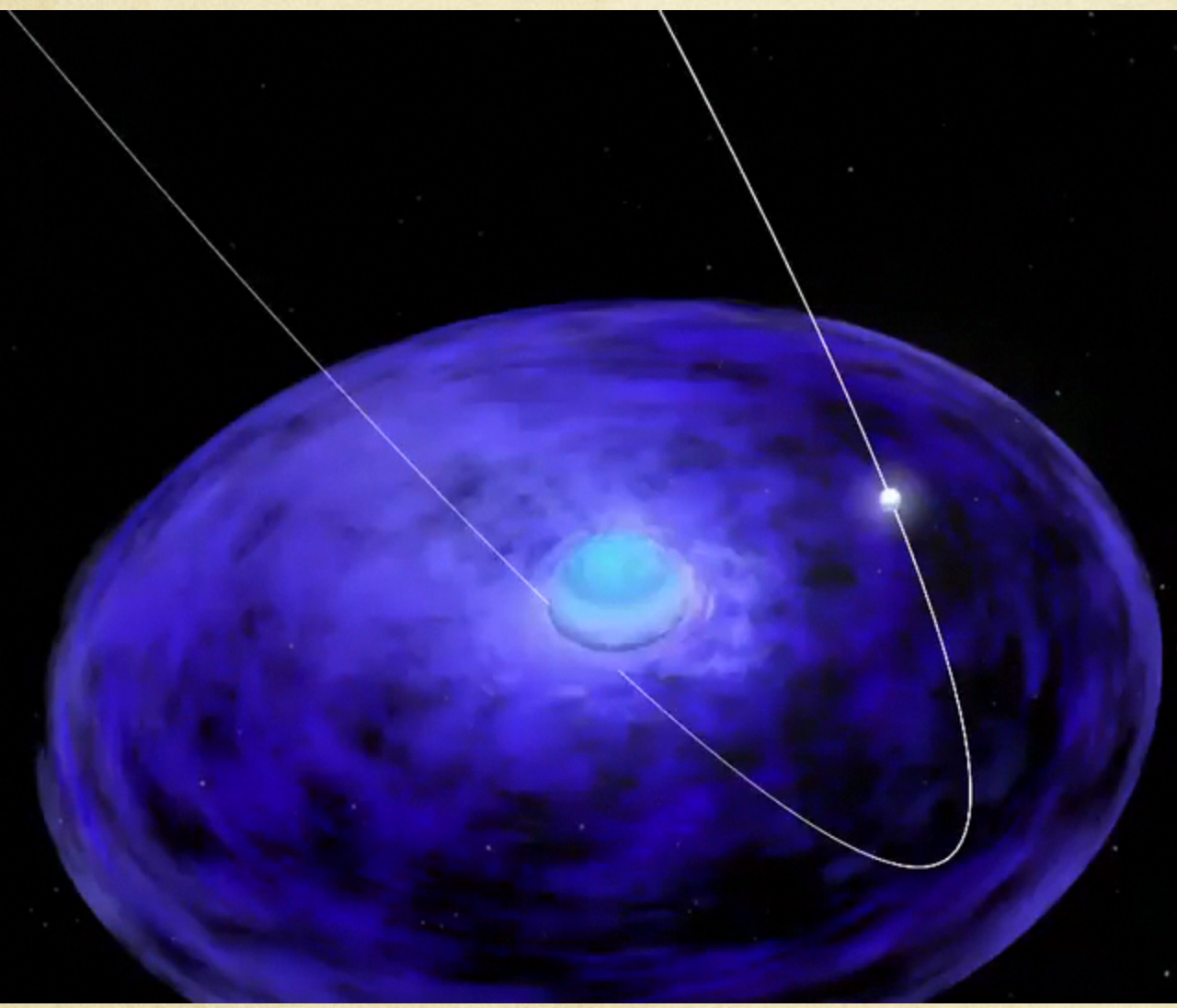
<sup>d</sup> Power-law photon index in the  $\sim$ 0.5–10 keV band.

<sup>e</sup> Anti-correlation between flux and photon index in the  $\sim$ 0.5–10 keV band.

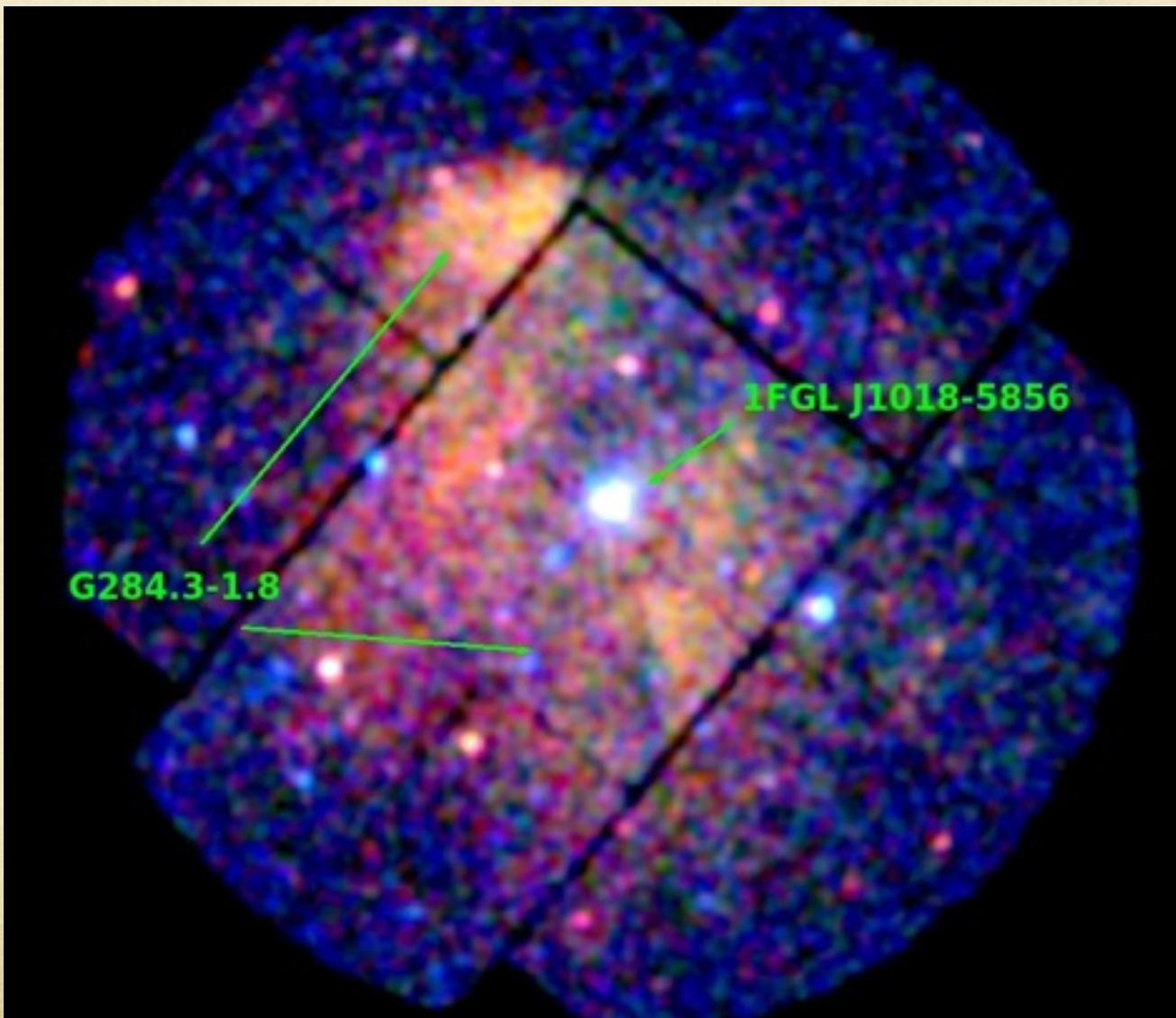
<sup>f</sup> Without five flares. See text for more details.

<sup>g</sup> Continuum is not modeled with a power law.

**References.** (1) Ackermann et al. 2012; (2) Li et al. 2011a; (3) Abramowski et al. 2012; (4) Paredes et al. 2000; (5) Takahashi et al. 2009; (6) Abdo et al. 2009a; (7) Aharonian et al. 2006; (8) Abdo et al. 2009b; (9) Li et al. 2011b; (10) Albert et al. 2006; (11) Harrison et al. 2000; (12) Tam et al. 2011; (13) Aharonian et al. 2005; (14) Johnston et al. 1992; (15) Kaspi et al. 1995; (16) Watanabe et al. 1994; (17) Abdo et al. 2009c; (18) Sinitzyna et al. 2011; (19) Hinton et al. 2009; (20) Skilton et al. 2009; (21) Bongiorno et al. 2011; (22) Rea & Torres 2011. See also references therein.

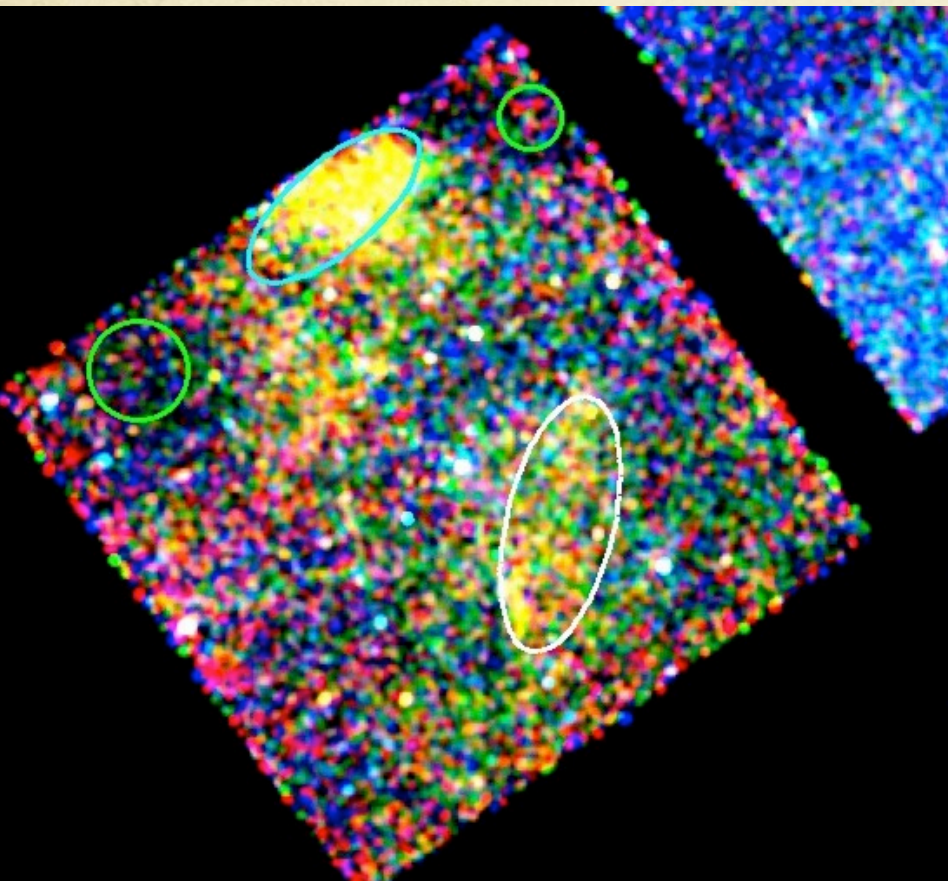


# G284 & J1018

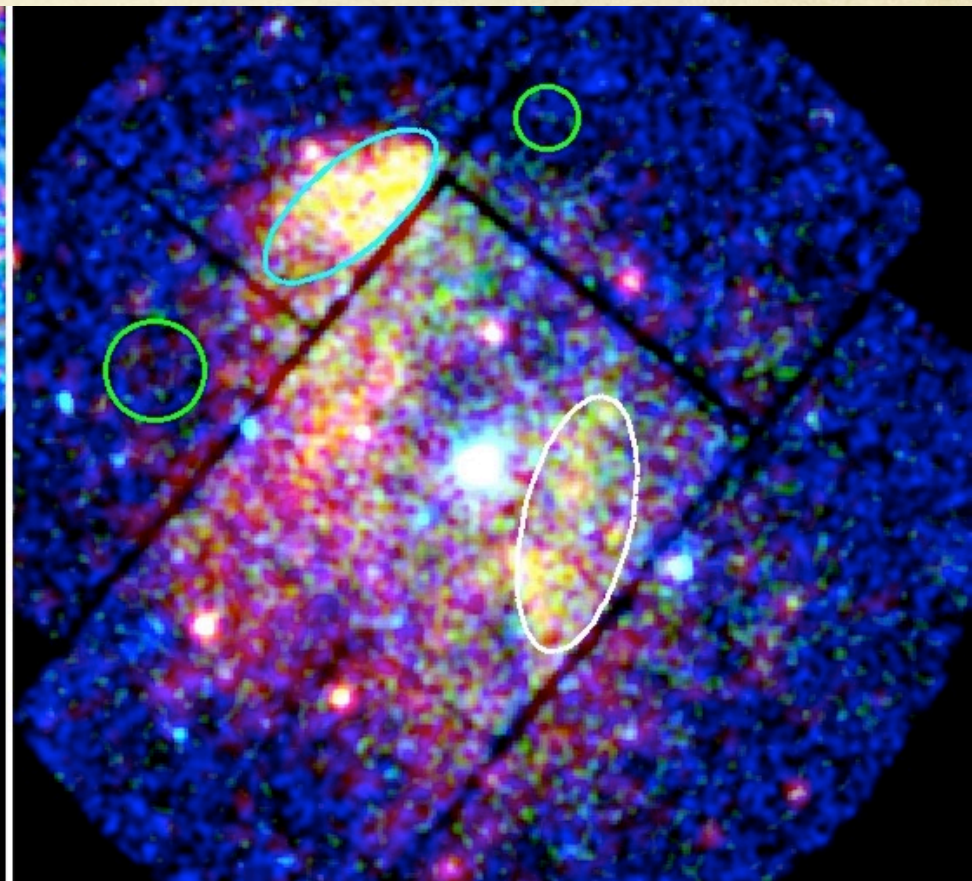




# G284



72 ks Chandra Obs. (ours)



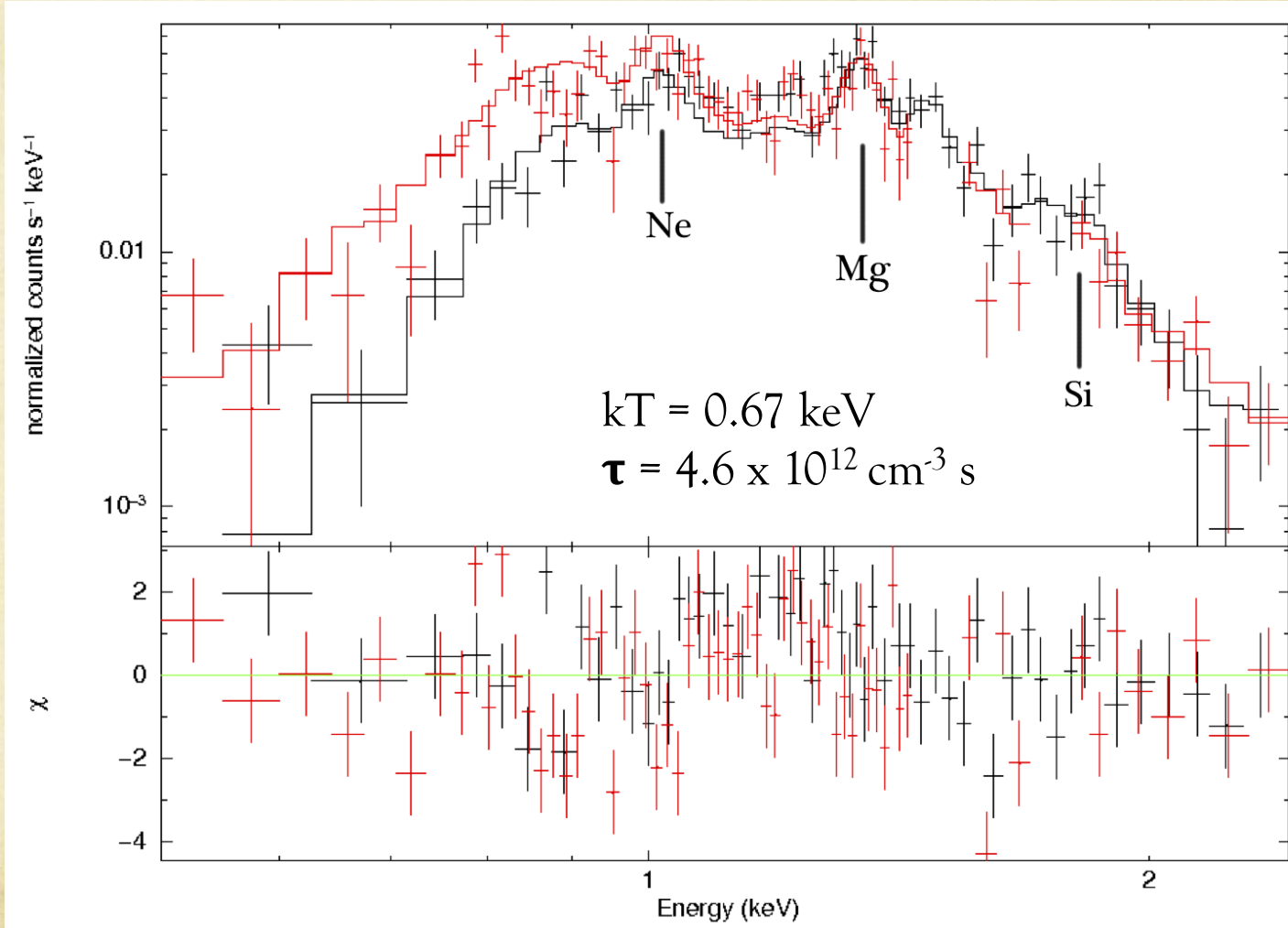
105 ks XMM Obs. (PI: De Luca)

# North Region

Model:  
 $pabs \times vpshock$

Abundances:

O=1  
Ne = 1.19  
Mg = 1.06  
Si = 0.19  
Fe = 0.24



# West Region

Model:  
 $pabs \times vpshock$

Abundances:

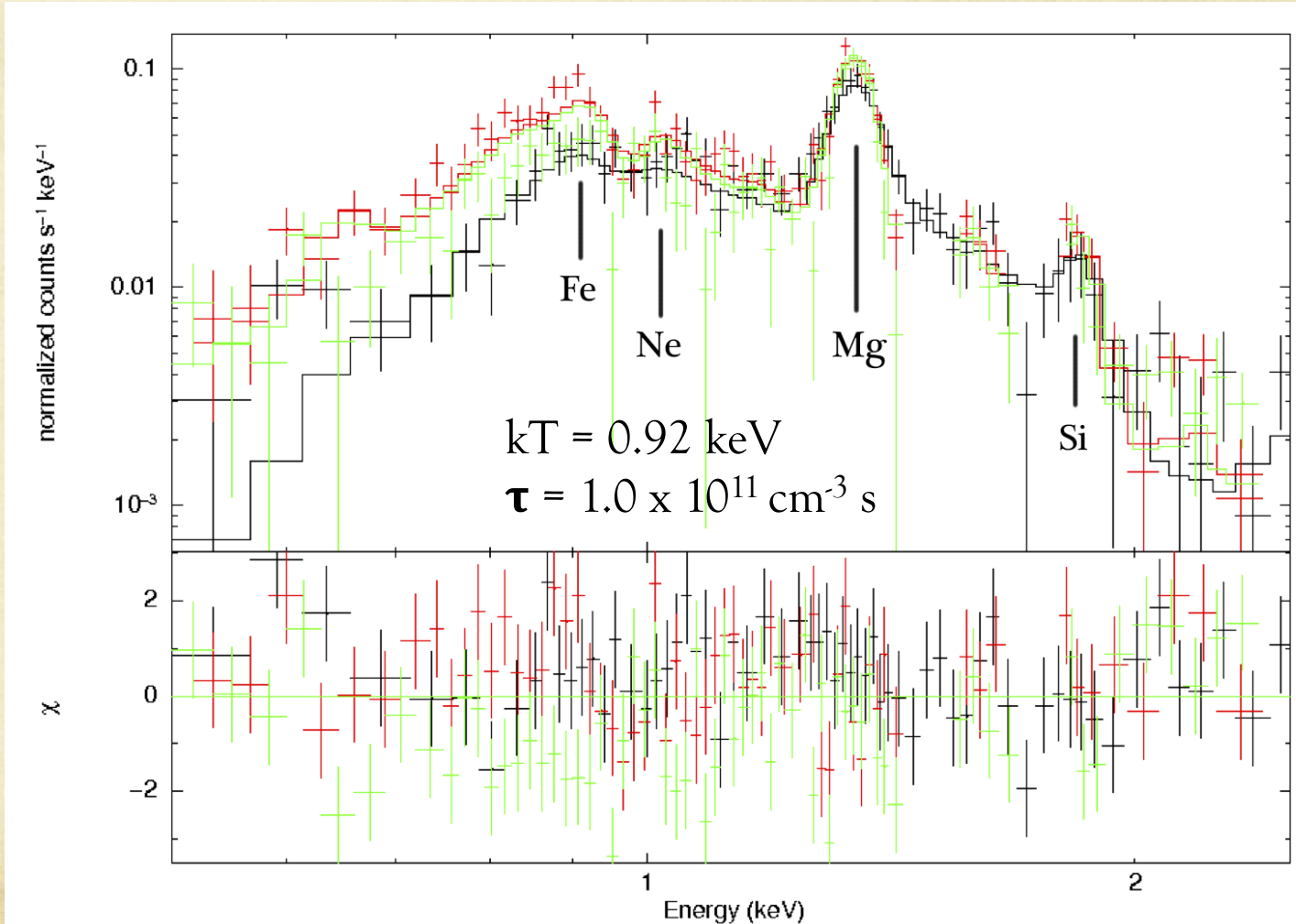
O=1

Ne = 1.30

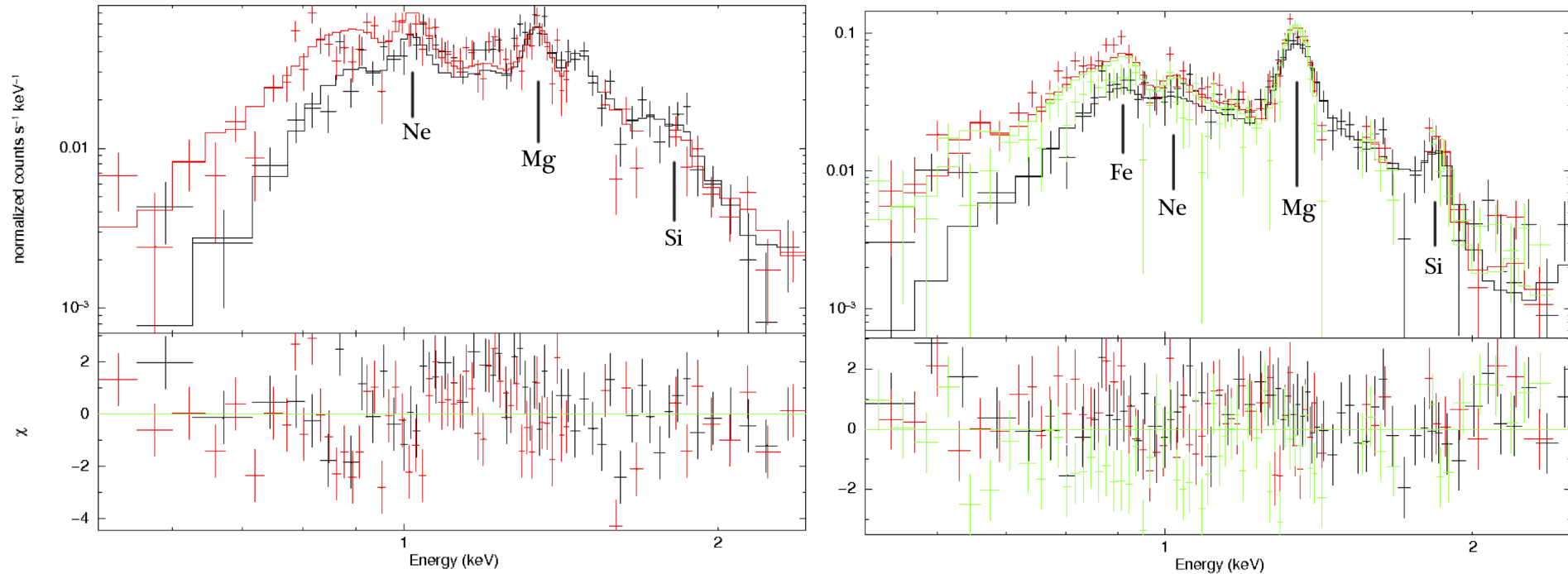
Mg = 4.53

Si = 1.50

Fe = 0.97

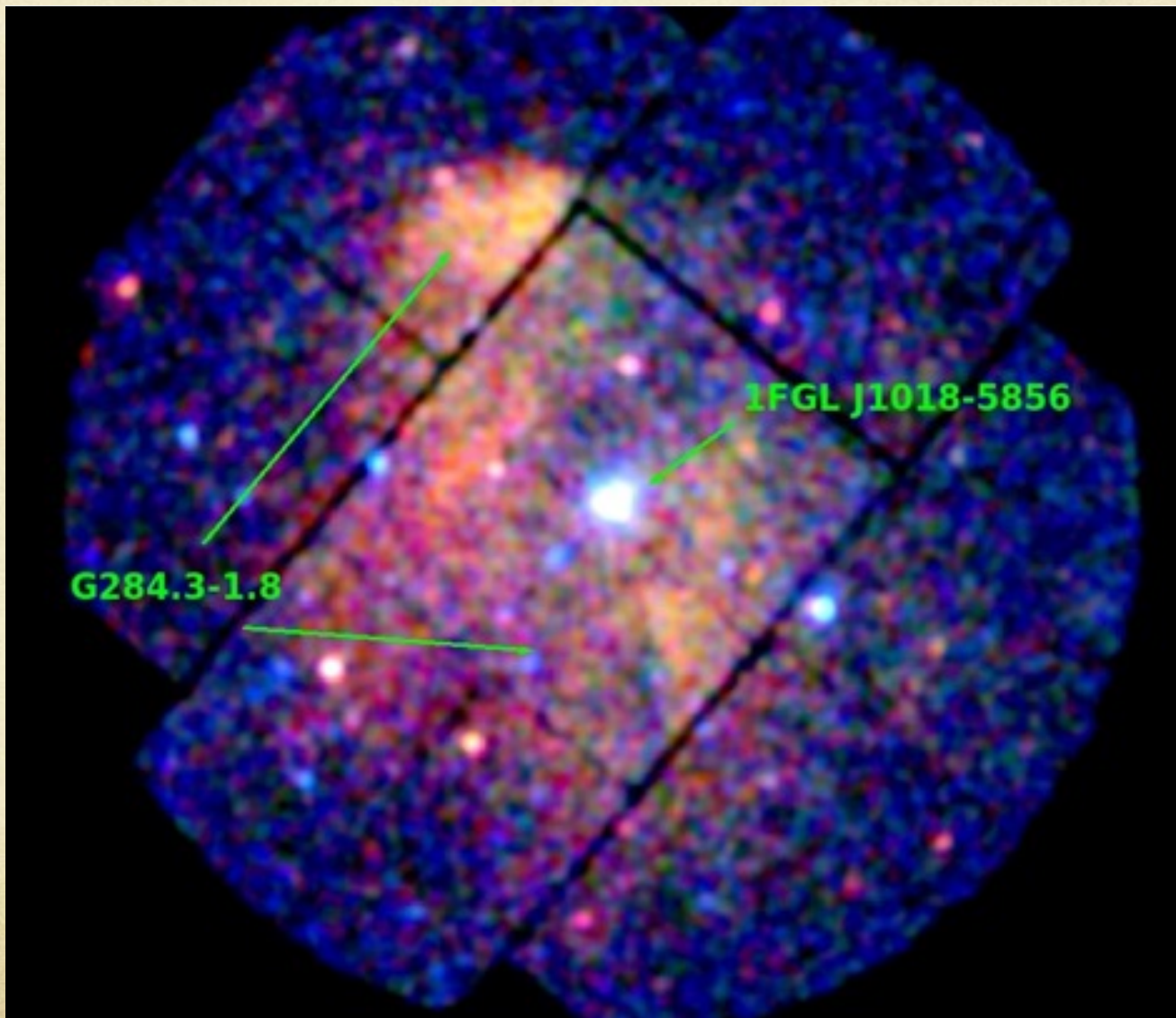


Chandra, XMM MOS 1, XMM MOS 2



- West region rich in Mg, spectra and abundances similar to N49B in LMC (Park et al. 2003), another SNR with Mg-rich ejecta.
- Nucleosynthesis models produce significant amounts of Mg in explosions of massive ( $> 25 M_{\odot}$ ).

# 1FGL J1018



# 1FGL J1018

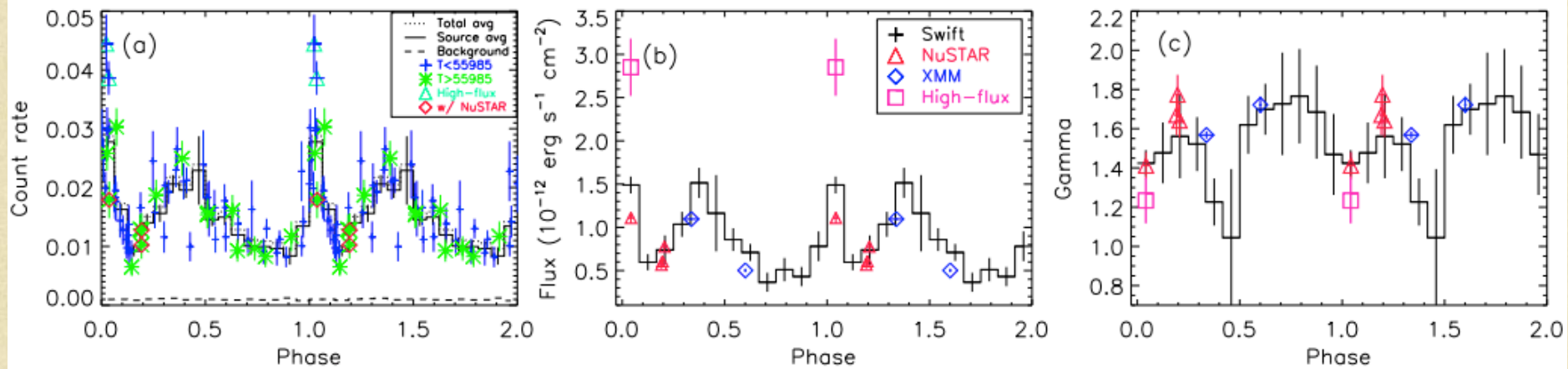
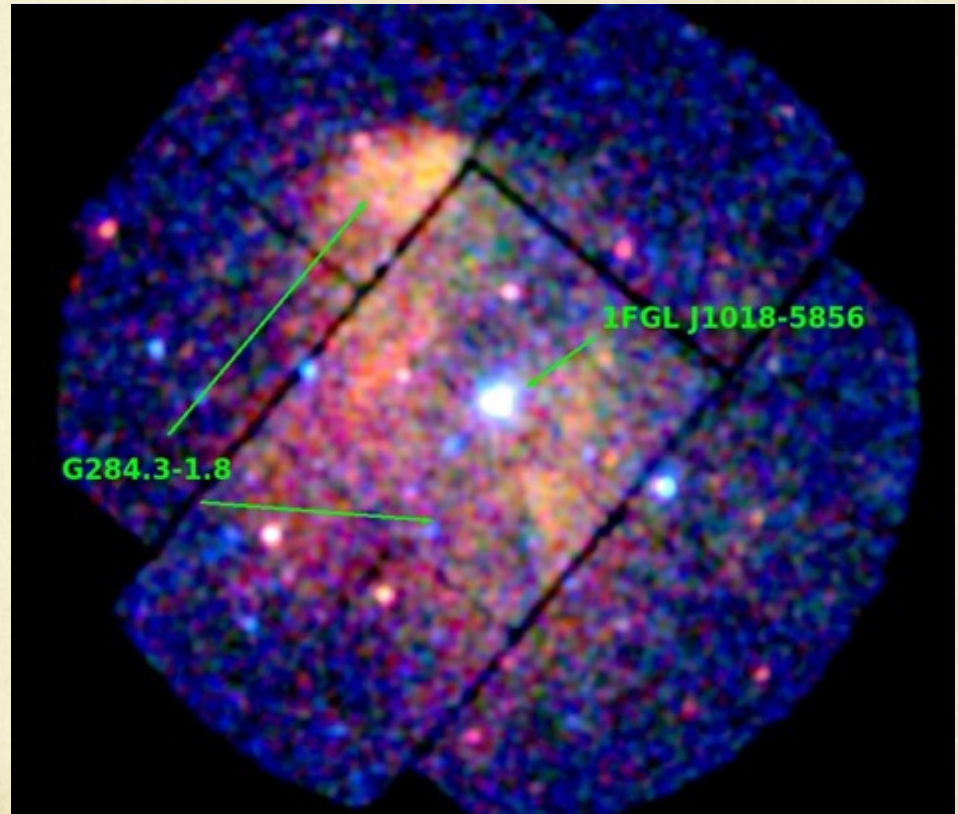


**Figure 2.** X-ray light curve and the best-fit spectral parameters for a power-law model. Only *Swift* data are shown in panel (a) and measurements made with all three instruments are shown in panels (b) and (c). *a)* 0.5–10 keV light curve as measured with *Swift*. Black dotted line shows the average count rate, black solid line is for the average source count rate, and the black dashed line shows the average background count rate. Blue data points are measurements reported by (before 55985 MJD An et al. 2013), and green data points are new measurements (Coley et al. 2014, and this work). Cyan triangle denotes the “high-flux state”, two observations which had significantly larger count rates than the others at the same phase, and red diamonds are for time periods in which *NuSTAR* observations were made. *b)* 3–10 keV flux corrected for interstellar absorption. Data points for *Swift*, *NuSTAR*, and the *XMM-Newton* measurements are denoted in cross, triangle, and diamond, respectively. *c)* the best-fit photon index. Same symbols as in (b) are used in (c).

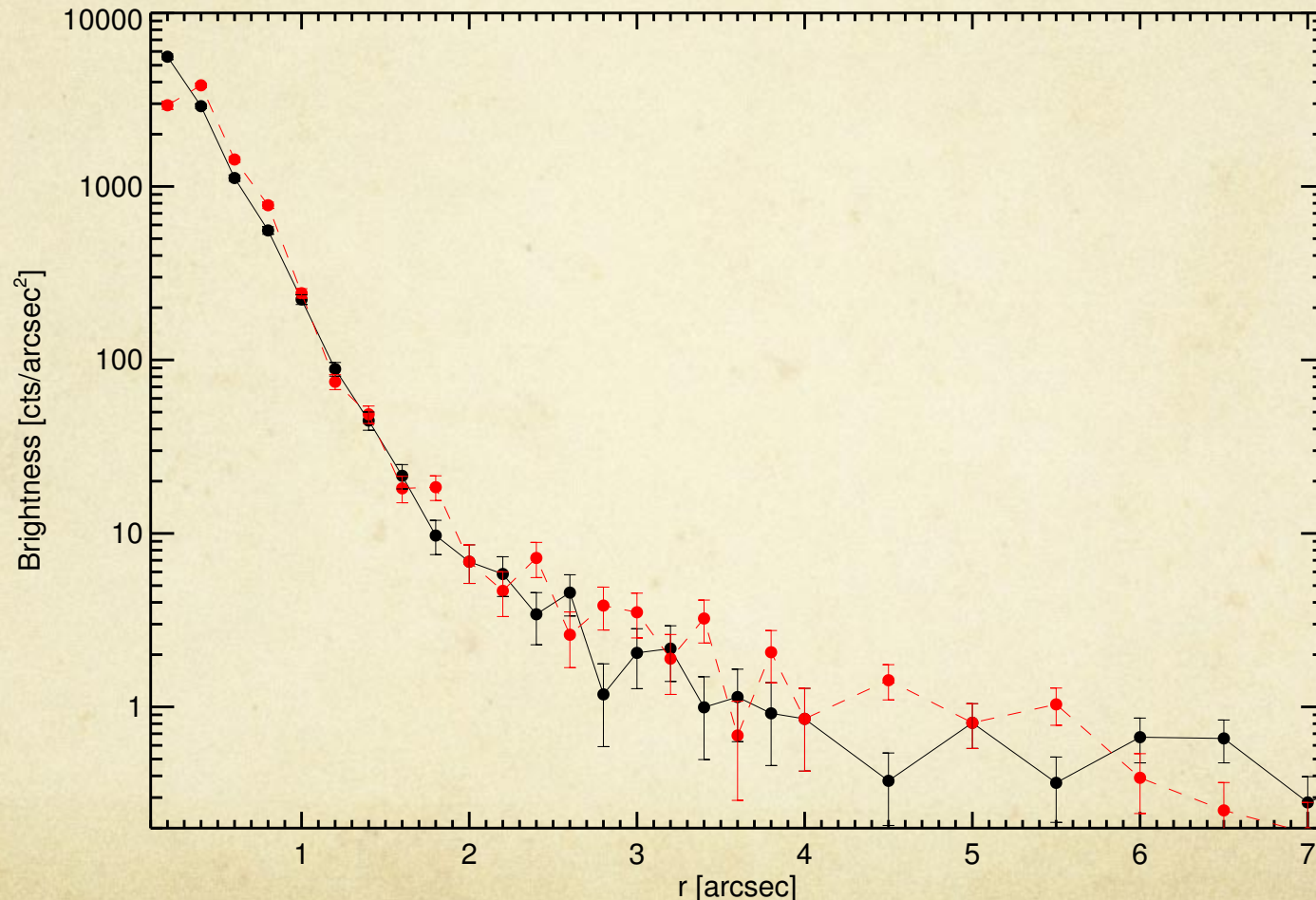
An et al. (2015)

# 1FGL J1018

- Chandra observations at binary phase 0.42 and 0.67.
- Power-law spectrum:
  - $nH = 9 \times 10^{21} \text{ cm}^{-2}$
  - $\Gamma \approx 1.75$
- It's a binary:
  - 16.6 d period
- Optical counterpart
  - O6V((f)) star
  - $M=30 M_{\odot}$
- One of only two high-mass  $\gamma$ -ray binaries inside an SNR (SS 433 in W50).

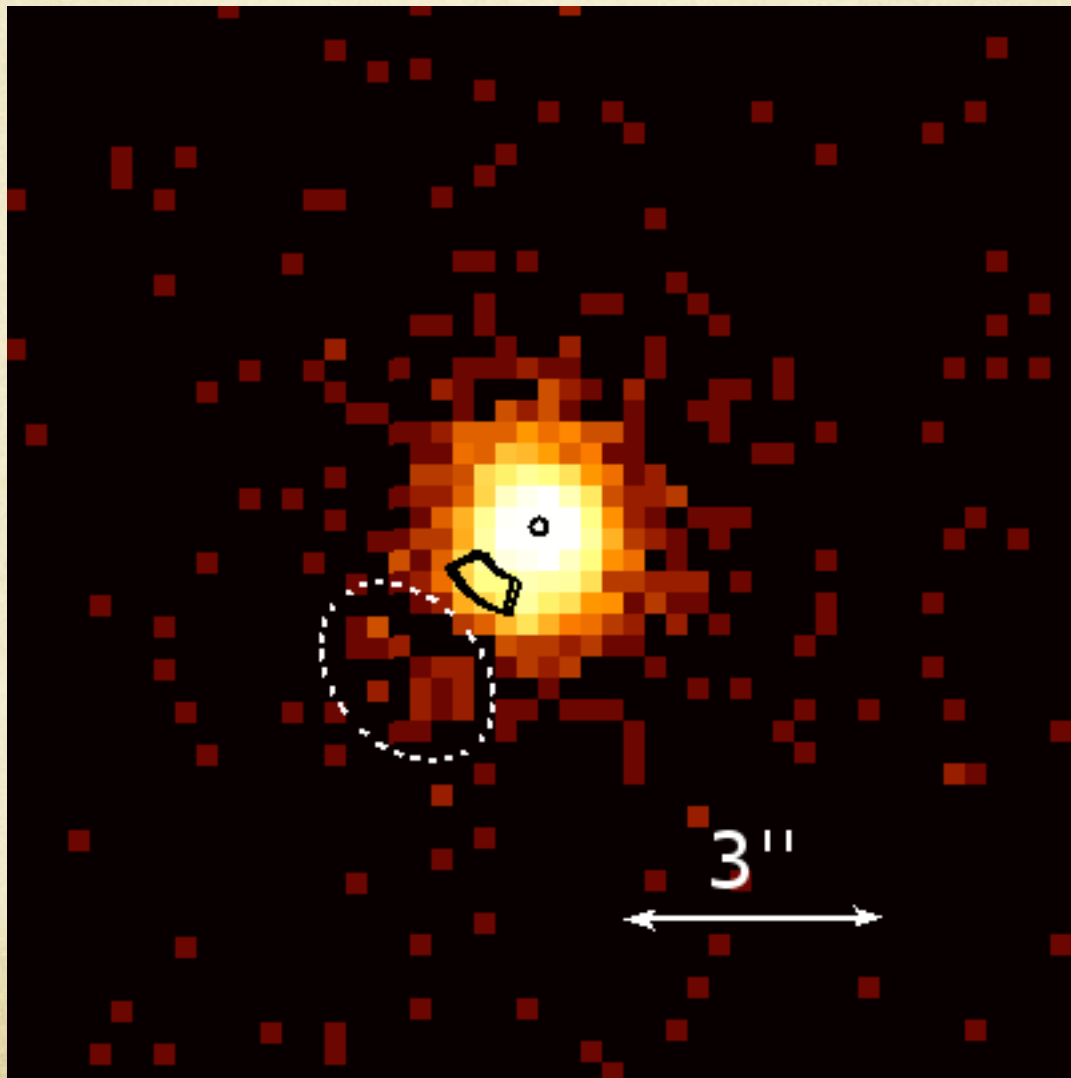


# Point Source Analysis

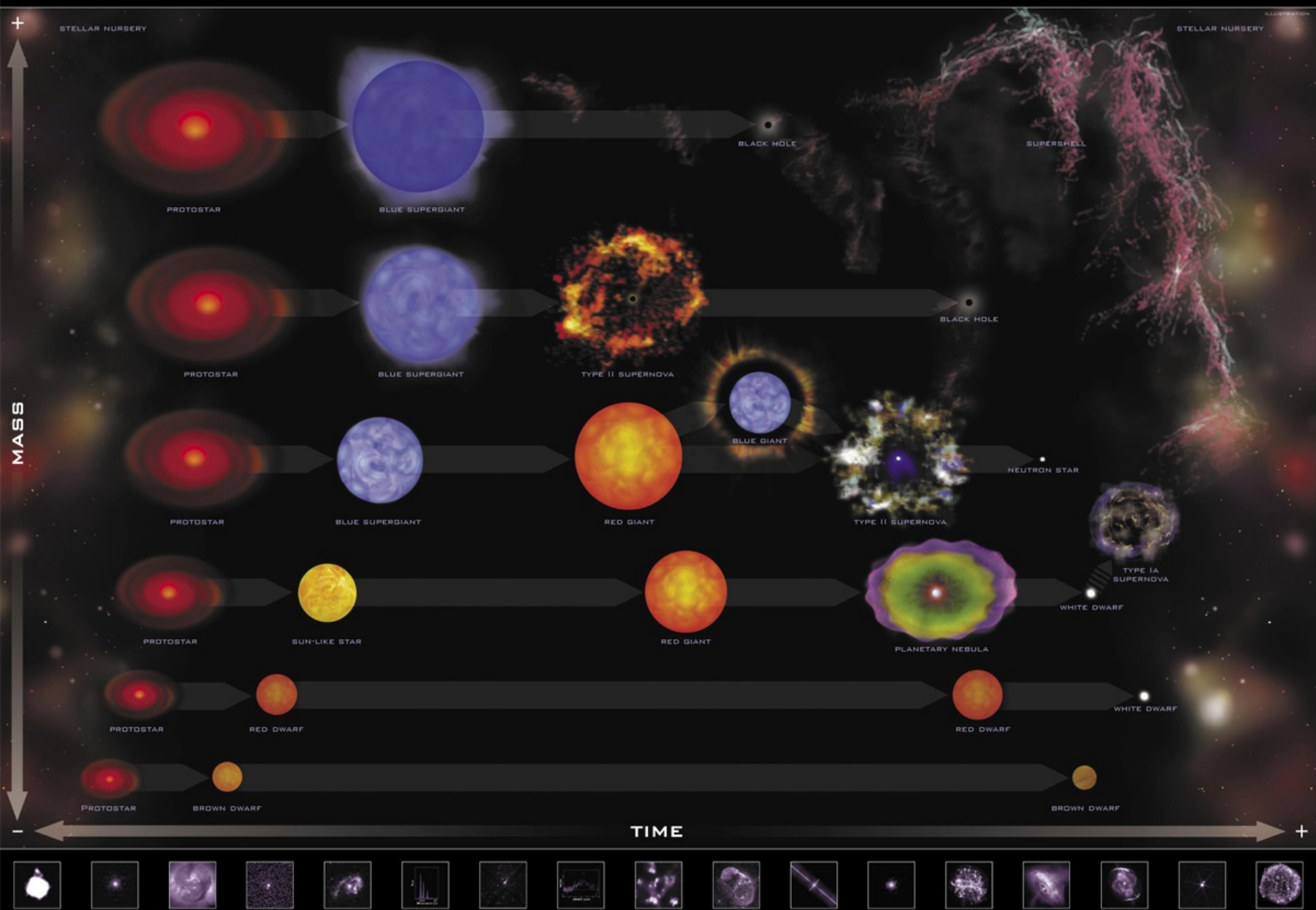


Profile vs. PSF model

# Point Source Analysis



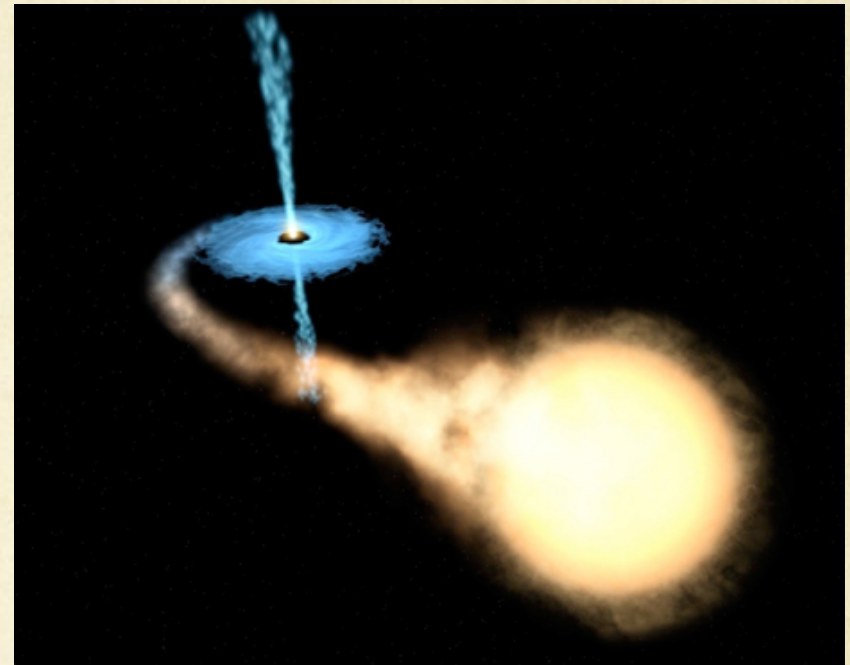
# STELLAR EVOLUTION: A JOURNEY WITH CHANDRA



# Binary Evolution

- Binary evolution code (Hurley+ 2002)

- Grid of 80,000 simulations:
  - $M_1 = 10\text{-}35 M_\odot$ ,  $M_2 = 12\text{-}50 M_\odot$ ,  
 $M_2 > M_1$ .
  - $P=5\text{-}50 \text{ d}$ ,  $e = 0\text{-}0.9$ .



- Best-fit reproduction with  $M_1 = 13.4 M_\odot$ ,  $M_2 = 26.7 M_\odot$ ,  $P = 18 \text{ d}$ ,  $e = 0.57$ .
- Results in  $2.2 M_\odot$  NS.

# Summary

- SNRs can reveal information about the progenitor system.
- 1FGL J1018.6-5856 has a power-law spectrum.
- Hint of extended emission.
- Ejecta in SNR appear Mg-rich, very similar to LMC SNR N49B
- Nucleosynthesis models favor massive stars  $> 25 M_{\odot}$ .
- Binary evolution models consistent with a heavy neutron star as compact object.; SN progenitor  $\simeq 27 M_{\odot}$ .